Eur. Phys. J. D **13**, 187–194 (2001)

THE EUROPEAN PHYSICAL JOURNAL D

EDP Sciences

Investigation of the hyperfine structure of Ta I lines (V)

B. Arcimowicz[1,a], A. Huss[1], S. Roth[1], N. Jaritz[1], D. Messnarz[2], G.H. Guthöhrlein[2], H. Jäger[1], and L. Windholz[1,b]

[1] Institut für Experimentalphysik, Technische Universität Graz, Petersgasse 16, 8010 Graz, Austria
[2] Labor für Experimentalphysik, Universität der Bundeswehr Hamburg, Holstenhofweg 85, 22043 Hamburg, Germany

Received 27 June 2000 and Received in final form 23 August 2000

Abstract. We report on further investigations of the hyperfine structure of spectral lines of the neutral tantalum atom. Besides determination of the hyperfine constants A and B of 21 levels we report on the discovery of 9 up to now unknown fine structure levels for which we could determine their energy position, parity, angular momentum and the constants A and B. For a large number of up to now unclassified lines the combinations could be identified.

PACS. 32.10.Fn Fine and hyperfine structure

1 Introduction

Earlier investigations of the hyperfine structure of the Ta atom have been performed by our groups [1–7] and others [9–21]. The Ta I spectrum was analyzed by Klinkenberg *et al.* [22] and van den Berg *et al.* [23]. In the standard tables of energy levels, published by Moore [24], Ta energy levels together with its configurations and designations are summarized, mainly based on the (unpublished) analysis of Kiess and Kiess and on references [22, 23]. Although many lines were classified in [22,23] and in the NBS tables [25], several lines in standard wavelength tables [26,27] remain unclassified. Moreover, on spectral plates exposed by the light of an Ar–Ta hollow cathode using an Ebert monochromator with 2 m focal length in fifth order, we found a large number of Ta spectral lines for which the wavelengths are not reported in standard wavelengths tables [26,27]. In this work a number of such lines have been excited by laser light.

During the course of investigations, we first concentrated only on the hyperfine constants of the classified lines [1–4,6]. Later on, we were able to use the large number of known pairs of hyperfine constants as a "fingerprint" for the levels, and by exciting unclassified lines and analyzing their hyperfine structure we turned over more and more to perform fine structure investigation by means of hyperfine structure spectroscopy [5,7,8]. In this way a large number of up to now unknown levels could be discovered, and a lot of spectral lines could be classified.

[a] *Permanent address:* Katedra Fizyki Atomowej, Politechnica Poznanska, 60-965 Poznan, Poland.
[b] e-mail: windholz@iep.tu-graz.ac.at

2 Experiment

The experimental arrangement is the same as in earlier works [1,5,8]. Free tantalum atoms were produced in a hollow cathode discharge by cathode sputtering, using Ar or Ne (or a proper mixture) as carrier gas. This source not only produces Ta atoms in the ground state but also in high lying excited states with populations sufficient for laser excitation. The discharge volume was exited by laser light generated by a tunable cw dye laser (4 190–7 000 Å) or a tunable cw Ti:sapphire laser (7 000–8 941 Å). UV excitation (3 295 Å) was performed by frequency doubling laser radiation in an external ring cavity. The cw laser light was chopped and the laser-induced fluorescence light was dispersed by a grating monochromator and detected with a photomultiplier using a lock-in amplifier. The optogalvanic signal could also be detected. For an accurate determination of the wavelengths of fluorescence lines, we used a second chopper with a much higher chop frequency directly before the entrance slit of the monochromator. In this way, besides the laser-induced fluorescence signal, the hollow cathode spectrum could be recorded as a wavelength reference, when setting the laser wavelength to a strong hyperfine component of the excitation line and scanning the transmission wavelength of the monochromator. The experimental setup is shown in Figure 1, an example of such a spectrum in Figure 2.

3 Results and discussion

For selecting lines to be investigated, we have taken a spectrum of a Ta–Ar hollow cathode lamp, using a 2 m grating spectrograph in fifth order. Figure 3a shows a small section of such a spectrum, around the line $\lambda = 4\,200.11$ Å. Besides well-known lines of Ta, listed in commonly used

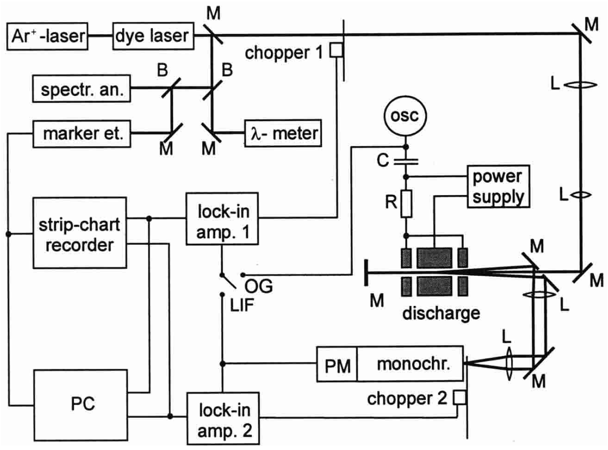

Fig. 1. Experimental setup. M: mirrors, B: beam splitters, L: lenses.

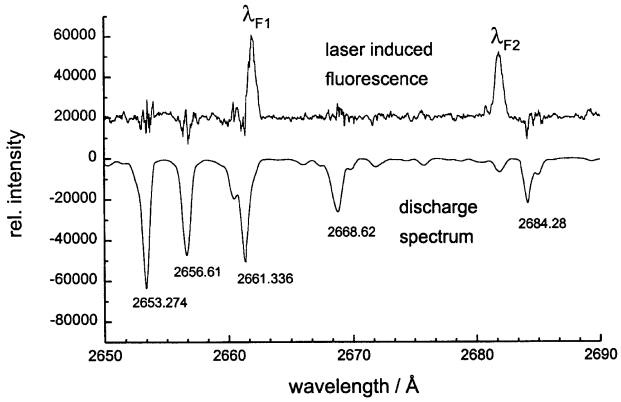

Fig. 2. Laser-induced fluorescence signal (upper trace) and fluorescence signal of the discharge when exciting the line $\lambda = 4\,244.88$ Å (the discharge spectrum has been inverted to make a comparison easier).

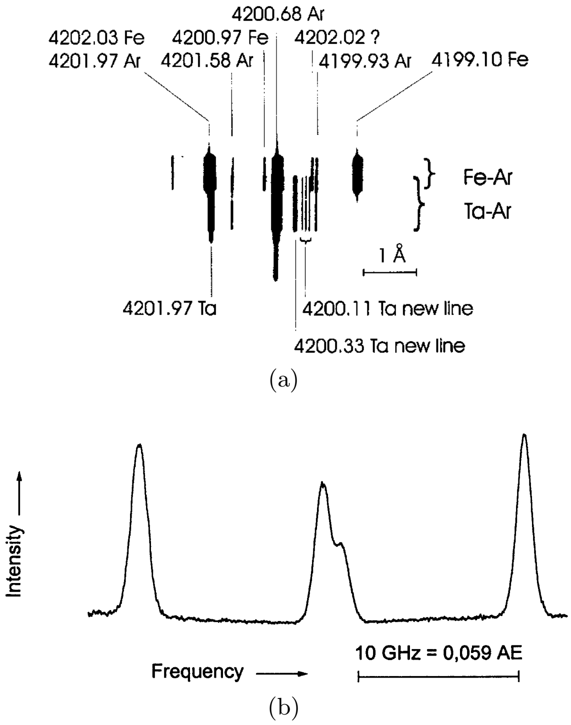

Fig. 3. (a) Part of the spectrum taken by the grating spectrograph. The line $\lambda = 4\,200.33$ Å is treated in a forthcoming paper. (b) Optogalvanic spectrum of the line $\lambda = 4\,200.11$ Å.

spectral tables [26,27], we have found a large number of additional lines. By exciting such lines, evaluating their hyperfine structure and searching for fluorescence lines, we were in most cases able to show without doubt that these lines belong to the neutral Ta atom. All wavelengths given in this paper are given in unit Å in air.

In Table 1 all investigated lines are listed. Each of the corresponding transitions was excited by laser light. When the wavelength is listed in [26] and/or [27], in column 2 the intensity from [26,27] is given. In cases of lines discovered on our spectral plate we give the remark *nl* (new line), the wavelength evaluated from the spectral plate (calibrated by means of an Ar–Fe spectrum) and an estimated intensity, using as a scale neighboured lines listed in [26]. Sometimes several hyperfine components can clearly be distinguished in the photographic spectrum. Some wavelengths above 6 934 Å have been calculated from the level energies, and we tried to excite the corresponding transitions. Successful cases are listed in Table 1, but no intensity entry can be given since the lines are outside the region of our spectral plates. For some of the investigated lines we present another classification as in other papers. In some of such cases we cannot exclude that the older classification is valid too, so we may have blend situations (where lines are overlaid).

When exciting the transitions listed in Table 1, the upper levels decay by emission of fluorescence lines, which show intensity modulation due to chopping the exciting laser light. While tuning the laser wavelength, the laser-induced fluorescence intensity was recorded and allows to evaluate the hyperfine structure of the excitation line (note that all fluorescence lines stemming from the same upper level show the structure of the excitation line). In most cases the fluorescence lines have been classified earlier. But several fluorescence lines could be classified for the first time; such lines are listed in Table 2. For the lines where no intensity is given, the wavelength is outside the range of our photographic spectra and is therefore calculated from the level energies. Here the same as before is valid as before in case of blend situations.

In Table 3 the A and B values of the investigated levels are listed, evaluating either laser-induced fluorescence signals or (in few cases) optogalvanic signals (if they show a better signal-to-noise ratio). If we have determined the constants on different lines, we give a mean value.

The investigation of some of the lines listed in Table 1 has lead us to the discovery of several new levels, for which we could determine energy, angular momentum, parity, A and B (Tab. 4). Two of these levels (20 144.81 cm^{-1} and 30 542.35 cm^{-1}) have been mentioned already in reference

Table 1. Investigated lines of Ta I.

λ/Å	Int. [27]/[26]	Transition even level	odd level	Level energy / cm^{-1} even	odd	Remark
3 295.326	140/125	$a\,^6D_{5/2}$	$y\,^6F^\circ_{5/2}$	11 243.63	41 580.98	
4 191.161 + 4 191.26	85/5 + −/3	$a\,^4P_{1/2}$	$y\,^6D^\circ_{1/2}$	60 49.42	29 902.27	new center wavelength
4 200.11	*nl* 25	$a\,^6D_{1/2}$	$?^\circ_{1/2}$	97 58.97	33 561.28	new line
4 241.05	*nl* 1	$4D_{1/2}{}^*$	$?^\circ_{1/2}$	20 144.81	43 717.15	new line
4 244.83		$^4D_{5/2}{}^*$	$z\,^6D^\circ_{3/2}$	48 290.45	24 739.03	
4 244.88	*nl* 2	$^2H_{9/2}{}^*$	$?^\circ_{11/2}$	29 116.26	52 667.30	new lower and upper level
4 244.90		$^4G_{7/2}{}^*$	$?^\circ_{9/2}$	24 917.90	48 468.96	
4 280.467	−/10	$a\,^4F_{3/2}$	$z\,^6F^\circ_{1/2}$	0	23 355.41	
4 284.49	*nl* 1	$a\,^4H_{11/2}$	$?^\circ_{9/2}$	22 428.56	45 762.01	new line, new upper level
4 319.28	*nl* 80	$a\,^4F_{9/2}$	$?^\circ_{9/2}$	5 621.04	28 766.65	new line
4 327.76	*nl* 1	$a\,^4G_{9/2}$	$?^\circ_{7/2}$	23 912.89	47 013.02	new line
4 349.78	*nl* 10	$a\,^6D_{7/2}$	$?^\circ_{9/2}$	12 234.76	35 217.94	new line
4 364.838	45/15	$a\,^4H_{7/2}$	$?^\circ_{5/2}$	20 646.54	43 550.78	
4 398.88	*nl* 5	$?_{9/2}{}^f$	$?^\circ_{11/2}$	50 509.7	27 783.00	new line
4 417.44	*nl* 10	$?_{7/2}{}^f$	$?^\circ_{9/2}$	47 817.16	25 185.89	new line
4 447.33	*nl* 5	$^4G_{7/2}{}^*$	$?^\circ_{5/2}$	24 917.90	47 397.06	new line
4 452.43	*nl* 1	$a\,^4D_{1/2}$	$y\,^4P^\circ_{3/2}$	22 235.97	44 689.31	new line
4 475.80	*nl* 5	$a\,^4H_{7/2}$	$?^\circ_{5/2}$	20 646.54	42 982.8	new line
4 496.18	*nl* 5	$^6D_{3/2}{}^*$	$?^\circ_{5/2}$	10 950.22	33 184.97	new line
4 534.40	*nl* 50	$^4D_{3/2}{}^*$	$y^4P^\circ_{5/2}$	24 275.95	46 323.31	new line
4 557.24	*nl* 3	$a\,^4H_{9/2}$	$?^\circ_{9/2}$	21 153.33	43 090.28	new line
4 846.810	−/10	$a\,^4H_{13/2}$	$?^\circ_{11/2}$	23 514.86	44 141.31	
4 861.043	−/3	$^2H_{9/2}{}^*$	$?^\circ_{11/2}$	29 116.26	49 682.23	
4 866.54	*nl* 0	$a\,^4D_{1/2}$	$?^\circ_{3/2}$	22 235.97	42 778.70	new line
4 873.01	*nl* 0	$^2I_{11/2}{}^*$	$?^\circ_{9/2}$	29 498.60	50 014.07	new line
4 923.21	*nl* 0	$^4G_{5/2}{}^*$	$?^\circ_{3/2}$	23 512.34	43 818.63	new line
5 064.612	−/7	$a\,^4G_{11/2}$	$?^\circ_{9/2}$	26 022.74	45 762.01	
5 517.665[e]	−/2	$a\,^4G_{11/2}$	$?^\circ_{11/2}$	26 022.74	44 141.31	
5 540.44	*nl* 1	$^2H_{9/2}{}^*$	$?^\circ_{9/2}$	29 116.26	47 160.34	new line
5 773.19	*nl* 0	$^4D_{1/2}{}^*$	$?^\circ_{1/2}$	20 144.81	37 461.46	new line
5 830.49	*nl* 1	$^4F_{5/2}{}^*$	$?^\circ_{3/2}$	24 546.20	41 692.64	new line
5 846.31	*nl* 0	$a\,^4H_{9/2}$	$?^\circ_{7/2}$	21 153.33	38 253.39	new line, blend
5 846.31	*nl* 0	$^4G_{7/2}{}^*$	$?^\circ_{7/2}$	24 917.90	42 017.95	new line, blend
5 846.86	*nl* 0	$?_{3/2}{}^f$	$z\,^4P^\circ_{1/2}$	43 964.50	26 866.05	new line
5 857.64	*nl* 1	$a\,^4D_{3/2}$	$y\,^4F^\circ_{5/2}$	21 381.01	38 447.99	new line
5 867.35	*nl* 0	$^4F_{5/2}{}^*$	$?^\circ_{5/2}$	24 546.20	41 584.94	new line
5 898.08	*nl* 80	$^2H_{11/2}{}^*$	$?^\circ_{9/2}$	33 064.154	50 014.07	new line
5 907.96	*nl* 0	$^4D_{3/2}{}^*$	$?^\circ_{3/2}$	24 275.96	41 197.67	new line
5 941.86	*nl* 0	$a\,^4G_{5/2}$	$y\,^4F^\circ_{5/2}$	21 622.92	38 447.99	new line
6 047.19[a]	*nl* 1	$^2H_{9/2}{}^*$	$?^\circ_{7/2}$	29 116.26	45 648.26	new line
6 170.46	24/−	$e\,^6F_{7/2}$	$?^\circ_{7/2}$	43 982.43	27 780.62	
6 170.538 + 6170.858	−/5 + −/8	$^4D_{1/2}{}^*$	$?^\circ_{1/2}$	20 144.81	36 345.8	new center wavelength
6 185.95	*nl* 1	$?_{9/2}$	$z\,^4H^\circ_{11/2}$	54 355.41	38 194.22	new line, new level
6 208.372[b]	24/10	$^4D_{5/2}{}^*$	$?^\circ_{3/2}$	27 715.66	43 818.63	classification
6 217.015[g]	−/8	$a\,^4D_{3/2}$	$?^\circ_{1/2}$	21 381.01	37 461.46	
6 221.34	*nl* 1	$?_{3/2}$	$z^2S^\circ_{1/2}$	36 409.65	20 340.39	new line, new level
6 228.015	*nl* 20	$^4H_{7/2}{}^*$	$z\,^4G^\circ_{9/2}$	22 761.21	38 813.32	new line

Table 1. *Continued.*

λ/Å	Int. [27]/[26]	Transition even level	odd level	Level energy / cm^{-1} even	odd	Remark
6 234.76	*nl* 1	$^4D_{1/2}{}^*$	$?^\circ_{3/2}$	26 743.95	42 778.7	new line
6 244.47	−/10	$^2I_{13/2}{}^*$	$?^\circ_{11/2}$	30 542.35	46 552.13	
6 247.322	−/2	$^4F_{3/2}{}^*$	$?^\circ_{1/2}$	22 842.84	38 845.25	classification
6 263.11	*nl* 1	$?_{3/2}$	$y\,^4D^\circ_{5/2}$	44 095.95	28 133.88	new line
6 271.36	*nl* 1	$^2H_{9/2}{}^*$	$?^\circ_{11/2}$	29 116.26	45 057.34	new line
6 274.297	−/3	$^4G_{9/2}{}^*$	$?^\circ_{5/2}$	24 917.90	40 851.61	
6 277.45	*nl* 0	$^4D_{5/2}{}^*$	$y\,^6F^\circ_{5/2}$	25 655.36	41 580.98	new line
6 281.334[c]	60/50	$e^6F_{5/2}$	$z^6F^\circ_{7/2}$	42 501.59	26 585.93	
6 417.99 + 6 418.477	−/2 + −/2	$^4D_{1/2}{}^*$	$?^\circ_{3/2}$	20 144.8	35 721.0	new center wavelength
6 418.48	−/2	$^4D_{1/2}{}^*$	$^4F^\circ_{3/2}$	20 144.81	35 721.0	
6 440.46	*nl* 2	$a\,^4G_{5/2}$	$?^\circ_{5/2}$	21 622.92	37 145.60	new line
6 453.113	−/3	$^4H_{7/2}{}^*$	$?^\circ_{7/2}$	22 761.21	38 253.39	classification confirmed
6 559.73	*nl* 0	$^4F_{5/2}{}^*$	$?^\circ_{5/2}$	24 546.20	39 786.52	new line
6 577.55	−/4	$a\,^4D_{3/2}$	$y\,^6F^\circ_{3/2}$	21 381.01	36 580.06	classification
6 578.75	−/2	$^4D_{5/2}{}^*$	$?^\circ_{5/2}$	25 655.36	40 851.61	
6 605.85	−/3	$^4G_{9/2}{}^*$	$z\,^4G^\circ_{11/2}$	25 376.41	40 510.38	classification
6 626.18	−/3	$^4D_{7/2}{}^*$	$?^\circ_{7/2}$	25 894.09	40 981.79	
6 639.41	−/2	$^2H_{9/2}{}^*$	$?^\circ_{9/2}$	29 116.264	44 173.62	classification
6 675.70	*nl* 50	$^2D_{3/2}{}^*$	$?^\circ_{5/2}$	25 876.05	40 851.61	new line
6 683.75	*nl* 0	$^4D_{7/2}{}^*$	$?^\circ_{5/2}$	25 894.092	40 851.61	new line
6 812.41	*nl* 0	$^2I_{11/2}{}^*$	$?^\circ_{9/2}$	29 498.604	44 173.62	new line
6 934.32	–	$^2H_{9/2}{}^*$	$?^\circ_{7/2}$	29 116.264	43 533.3	
6 971.31	8/–	$a\,^4G_{9/2}$	$?^\circ_{7/2}$	23 912.89	38 253.39	
6 977.67	−/2	$^2F_{5/2}{}^{**}$	$?^\circ_{7/2}$	44 918.665	30 590.95	
6 995.49	−/125	$a^4P_{1/2}$	$z\,^2S^\circ_{1/2}$	6 049.42	20 340.39	
7 002.54	–	$a\,^4D_{7/2}$	$?^\circ_{5/2}$	26 575.02	40 851.61	
7 003.10	−/2	$^2H_{9/2}{}^*$	$?^\circ_{9/2}$	29 116.26	43 391.71	
7 005.90	−/2	$^4D_{3/2}{}^*$	$?^\circ_{3/2}$	24 275.96	38 545.70	
7 016.42	–	$^4G_{5/2}{}^*$	$?^\circ_{3/2}$	23 512.34	37 760.67	
7 055.90	–	$^4D_{3/2}{}^*$	$y\,^6F^\circ_{5/2}$	27 412.36	41 580.98	
7 109.85	–	$^2H_{9/2}{}^*$	$y^6F^\circ_{7/2}$	29 116.264	43 177.37	
7 174.91	13/10	$^4D_{1/2}{}^*$	$?^\circ_{3/2}$	20 144.81	34 078.42	
7 277.54	5/3	$^4F_{3/2}{}^*$	$y\,^4F^\circ_{3/2}$	22 842.84	36 580.06	
7 351.43	–	$^2I_{13/2}{}^*$	$?^\circ_{11/2}$	30 542.35	44 141.31	
7 480.29	–	$?_{5/2}$	$?^\circ_{3/2}$	44 918.665	31 553.89	
7 650.42	−/2	$^4G_{5/2}{}^*$	$y\,^4F^\circ_{3/2}$	23 512.34	36 580.06	
7 818.73[d]	−/3	$?_{5/2}$	$?^\circ_{7/2}$	44 918.665	32 132.38	new classification
7 869.54	–	$^4F_{5/2}{}^{**}$	$?^\circ_{3/2}$	44 918.665	32 214.94	
7 929.92	–	$^6S_{5/2}{}^*$	$?^\circ_{5/2}$	32 502.382	45 109.37	
7952.07	5/3	$^2D_{3/2}{}^*$	$y\,^4F^\circ_{5/2}$	25 876.05	38 447.99	
7 996.56	–	$^2D_{3/2}{}^*$	$y^4P^\circ_{3/2}$	32 187.394	44 689.31	
7 997.76	–	$?_{3/2}$	$?^\circ_{1/2}$	49 961.515	37 461.46	
8 013.40	–	$^2H_{11/2}{}^*$	$?^\circ_{9/2}$	33 064.154	45 539.80	
8 041.60	–	$?_{5/2}$	$y^6D^\circ_{5/2}$	44 918.665	32 486.75	
8 088.85	–	$^4D_{7/2}{}^*$	$?^\circ_{7/2}$	25 894.092	38 253.39	

Table 1. *Continued.*

	Int.	Transition		Level energy / cm^{-1}		Remark
λ/Å	[27]/[26]	even level	odd level	even	odd	
8 199.47	–	$^2D_{5/2}{}^*$	$?^\circ_{5/2}$	32 916.837	45 109.373	
8 282.63	–	$^4D_{1/2}{}^*$	$?^\circ_{7/2}$	20 144.81	32 214.94	
8 670.82	–	$^2D_{3/2}{}^*$	$?^\circ_{1/2}$	32 187.394	43 717.15	
8 940.48	–	$^2I_{13/2}{}^*$	$?^\circ_{15/2}$	30 542.35	41 724.354	

If not marked otherwise, designations are taken from reference [24], * designation as given in reference [7], ** designation as given in reference [30], [a] blend situation with 6 047.25 Å [25], [b] up to now classified as 41 580.98–25 478.30 cm^{-1} [25], may be a blend situation, [c] blend situation with 26 866.05–10 950.22 cm^{-1} [2], as already stated by van den Berg *et al.* [23], [d] up to now classified as 28 689.31–15 903.77 cm^{-1} [22], may be a blend situation, [e] blend situation with 5 517.73 Å [8], [f] we think that the designations given in [24], e^4F, is wrong (see statements given in Ref. [8]), [h] in table [26], a Ta-line with 6 217.083 Å is listed, which could not be found on our spectral plates, *nl* this line shows up on spectral plates, given intensity is estimated. Intensity 0 means "just visible", – no intensity estimate can be given, since the wavelength is outside the range of our spectral plates. In these cases the wavelength given is calculated from the level energies.

Table 2. Lines classified *via* laser-induced fluorescence.

	Int.	Transition		Level energy / cm^{-1}		Excitation	Remark
λ / Å	[27]/[26]	even level	odd level	even	odd	λ / Å	
2 295.46	–	$a\,^4F_{3/2}$	$?^\circ_{5/2}$	0	43 550.78	4 364.838	
2 429.66	–/2	$a\,^4F_{7/2}$	$?^\circ_{5/2}$	3 963.92	45 109.373	7 929.92	
2 490.46	500/–	$a\,^4F_{9/2}$	$?^\circ_{9/2}$	5 621.04	45 762.010	5 064.612	
2 560.678	180/70	$a\,^4P_{3/2}$	$?^\circ_{5/2}$	6 068.91	45 109.373	7 929.92	
2 662.102	130/25	$a\,^2H_{11/2}$	$?^\circ_{11/2}$	15 114.14	52 667.3	4 244.88	
2 681.869	110/50	$a\,^2H_{9/2}$	$?^\circ_{11/2}$	1 5391.01	52 667.3	4 244.88	
2 845.450	–/8	$a\,^6D_{3/2}$	$?^\circ_{5/2}$	9 975.81	45 109.373	7 929.92	
3 022.286	–/3	$a\,^2H_{9/2}$	$?^\circ_{9/2}$	15 391.01	48 468.96	4 244.90	blend[a]
3 040.976	75/50	$a\,^6D_{7/2}$	$?^\circ_{5/2}$	12 234.76	45 109.373	7 929.92	
3 084.525	–/3	$a\,^6D_{9/2}$	$?^\circ_{9/2}$	13 351.45	45 762.01	4 284.49, 5 064.612	
3 209.73	–	$a\,^2G_{7/2}$	$?^\circ_{5/2}$	9 705.38	40 851.61	6 274.297	blend[b]
3 274.458	–/35	$a\,^4P_{1/2}$	$y^4F^\circ_{3/2}$	6 049.42	36 580.06	7 650.42	
3 361.71	–	$a\,^6D_{5/2}$	$?^\circ_{7/2}$	11 243.63	40 981.79	6 626.18	blend[c]
3 406.61	–	$a\,^6D_{7/2}$	$y\,^6F^\circ_{5/2}$	12 234.76	41 580.98	7 055.90	blend[d]
3 440.237	–/18	$a^2H_{11/2}$	$?^\circ_{9/2}$	15 114.14	44 173.62	6 639.41	
3 581.30	–	$^2P_{3/2}{}^*$	$?^\circ_{3/2}$	15 903.77	43 818.63	6 208.37	
3 592.495	–/2	$e^4F_{9/2}$	$z\,^6G^\circ_{9/2}$	50 509.7	22 681.71	4 398.88	
3 791.10	–	$a\,^6D_{3/2}$	$?^\circ_{1/2}$	9975.81	36 345.8	6 170.71	
3 947.74	–	$?_{9/2}{}^h$	$?^\circ_{9/2}$	50 509.7	25 185.89	4 398.88	
4 268.255	130/50	$e\,^6F_{7/2}{}^h$	$z\,^6G^\circ_{7/2}$	43 982.43	20 560.26	6 170.46	
4 789.24	–/4	$^4F_{3/2}{}^*$	$?^\circ_{1/2}$	22 842.84	43 717.154	670.82	blend[e]
4 958.114	18/8	$^4G_{9/2}{}^*$	$?^\circ_{9/2}$	25 376.41	45 539.801	8 013.40	
5 433.060	–/2	$^4D_{1/2}$	$?^\circ_{3/2}$	20 144.81	38 545.70	7 005.90	
6 147.087	–/15	$^2G_{7/2}$	$?^\circ_{9/2}$	29 276.388	45 539.801	8 013.40	blend[f]
6 578.94	–/2	$^2F_{5/2}{}^{**}$	$?^\circ_{7/2}$	44 918.665	29 722.95	6 977.67	blend[g]

If not marked otherwise, designations are taken from reference [24], * designation as given in reference [7], ** designation as given in [30], [a] blend with 3 022.26 Å, 43 768.55–10 690.32 cm^{-1} [23], [b] blend with 3 209.866 Å, 48 369.35–17 224.47 cm^{-1} [23], [c] blend with 3 361.64 Å, 43 090.28–13 351.45 cm^{-1} [22], this transition was observed when exciting the transition belonging to the line λ = 7 355.44 Å [8], [e] blend with 4 789.279 Å, 44 386.40–23 512.34 cm^{-1}, this transition was observed when exciting the transition belonging to the line λ = 8 412.34 Å [8], [f] blend with 6 147.07 Å, 45 762.01–29 498.60 cm^{-1}, this transition was observed when exciting the the transition belonging to line λ = 5 064.61 Å [this work], [d] this line may be a blend with the unclassified line 3 406.664 Å (intensity –/70), [g] blend with 6 578.78 Å, see Table 1, [h] we think that the designation given in [24], $e\,^4F$, is wrong (see statements given in Ref. [8]).

Table 3. A- and B-constants of the investigated levels.

Configuration	Designation	Energy / cm^{-1}	A / MHz	B / MHz	λ_{exc} / Å
even parity					
$5d^3 6s(a\,^5\mathrm{F})7s^{\mathrm{a}}$	$?_{9/2}{}^{\mathrm{a}}$	50 509.7	381(10)	874(50)	4 398.88
odd parity					
$5d^2\ 6s^2(a\,^3\mathrm{P})6p$	$z\,^2\mathrm{S}^{\circ}_{1/2}$	20 340.39	630.6(30)	0	6 221.34, 6 995.49
$5d^3\ 6s(a\,^3\mathrm{G})6p$	$y\,^4\mathrm{F}^{\circ}_{3/2}$	36 580.06	−899.1(15)	224(20)	6 577.55, 7 277.54
?	$?^{\circ}_{1/2}$	37 461.46	1 411.5(20)	0	5 773.19
?	$?^{\circ}_{7/2}$	38 253.39[b]	379.7(30)	876(40)	5 846.31, 6 971.31, 8 088.85
$5d^3\ 6s(a\,^3\mathrm{G})6p$	$y\,^4\mathrm{F}^{\circ}_{5/2}$	38 447.99	360.7(60)	−194(40)	5 941.86, 7 952.07
?	$?^{\circ}_{5/2}$	40 851.61	−125.2(20)	75(60)	6 578.75, 6 274.297
$5d^4(a\,^5\mathrm{D})6p$	$y\,^6\mathrm{F}^{\circ}_{5/2}$	41 580.98	−40(20)	−1 520(250)	3 295.326, 6 277.45
?	$?^{\circ}_{5/2}$?	41 584.94	361(30)	19(200)	5 867.35
?	$?^{\circ}_{3/2}$	41 692.64	281.8(20)	13(50)	5 830.49
?	$?^{\circ}_{7/2}$	42 017.95	309.7(20)	−637(50)	5 846.31
?	$?^{\circ}_{3/2}$	42 778.7	662.2(20)	60(10)	4 866.54, 6 234.76
$5d^4(a\,^5\mathrm{D})6p$	$y\,^6\mathrm{F}_{7/2}$	43 177.37	73.4(20)	237(30)	7 109.85
?	$?^{\circ}_{7/2}$	43 533.3	283.5(20)	532.5(30)	6 934.32
?	$?^{\circ}_{3/2}$	43 818.63	1 435.8(30)	352(10)	4 923.21, 6 208.372
?	$?^{\circ}_{11/2}$	44 141.31	252.2(30)	3 194(70)	4 846.810, 7 351.43
?	$?^{\circ}_{9/2}$	44173.62	646.6(15)	2424(15)	6 639.41, 6 812.41
$5d^4(a\ ^5\mathrm{D})6p$	$y\,^4\mathrm{P}^{\circ}_{3/2}$	44 689.31	−141.3(35)	511(20)	4 452.43
?	$?^{\circ}_{11/2}$	46 552.13	370.3(20)	584(50)	6 244.47
?	$?^{\circ}_{9/2}$	48 468.96	353(5)	1 500(50)	4 244.90
?	$?^{\circ}_{9/2}$	50 014.07	247.5(20)	1 992(50)	4 873.01, 5 898.08

Configurations and designations are taken from reference [24], [a] we think that the designation given in [24], e^4F, is wrong (see statements given in Ref. [8]). This level was treated in reference [6] as possible not existent, but the present investigations are confirming it is really existing, [b] hyperfine constants for this level (A = 374 MHz, B = 725 MHz) were already given in reference [6], here we present improved values.

Table 4. New energy levels.

Configuration	Designation	Energy / cm^{-1}	A/ MHz	B / MHz	λ_{exc} / Å
even parity					
$5d^4(^5\mathrm{D})6s$	$^4\mathrm{D}_{1/2}{}^*$	20 144.81	5 638.0(30)	0	5 773.19, 6 418.48, 7 174.91, 8 282.63
$5d^4(^3\mathrm{H})6s$	$^2\mathrm{H}_{9/2}{}^*$	29 116.26	690.0(20)	546(40)	6 047.19, 6 639.41, 7 003.10
$5d^4(^1\mathrm{I})6s$	$^2\mathrm{I}_{13/2}{}^*$	30 542.35	1 057.7(30)	2 745(60)	6 244.47, 7 351.43, 8 940.48
?	$?_{3/2}$	36 409.65	1207(5)	775(50)	6 221.34
?	$?_{9/2}$	54 355.41	195(5)	1 661(50)	6 185.95
odd parity					
?	$?^{\circ}_{1/2}$	43 717.15	−1121(10)	0	8 670.82
?	$?^{\circ}_{5/2}$	45 109.37	157.3(20)	−601(20)	7 929.92
?	$?^{\circ}_{9/2}$	45 539.80	609(2)	182(20)	8 013.40
?	$?^{\circ}_{9/2}$	45 762.01	599.5(40)	−720(70)	4 284.49, 5 064.612
?	$?^{\circ}_{11/2}$	52 667.30	124.3(50)	3 161(200)	4 244.88

* Configuration and designation as given in reference [7].

Table 5. Lines with new center of gravity wavelength.

Wavelength in [27] and/or [26]	New center wavelength / Å	Wavelengths of components (or component groups) / Å	Level energy / cm^{-1} J even	odd
		4 191.15	6 049.42	29 902.27
4 191.161	4 191.20	4 191.17	1/2	1/2
4 191.26		4 191.23		
		4 191.26		
		6 170.52	20 144.81	36 345.80
6 170.538	6 170.71	6 170.58	1/2	1/2
6 170.85		6 170.82		
		6 170.87		
6 417.99	6 418.27	6 418.08	20 144.8	35 721.0
6 418.477		6 418.42	1/2	3/2

[7] as new levels for comparison with theory, without giving any details.

Some of the spectral lines listed in [26] or [27] have been identified as belonging to the same transition but appearing as separated structures in the spectra due to the large hyperfine splitting. For these lines the new center of gravity wavelength is given in Table 5, together with the wavelengths of hyperfine components or hyperfine component groups.

We now are going to discuss several of the investigated problems in detail. Figure 2a shows a part of the spectrum gained with our spectrograph. Besides known lines, a triplet with its center wavelength of 4 200.11 Å is obvious. This line is not listed in the wavelength tables. We could identify it as the transition

$$a^6\mathrm{D}_{1/2}\ (9\,758.97\ \mathrm{cm}^{-1}) - ?^\circ_{1/2}\ (33\,561.28\ \mathrm{cm}^{-1})$$

by calculating wave number differences within the manifold of known levels. The hyperfine pattern of this line could be obtained when scanning the laser wavelength around 4 200.1 Å while recording the fluorescence intensity of the line 2 978.75 Å (having as its upper level $?^\circ_{1/2}$, 33 561.28 cm^{-1}), and also using optogalvanic detection (see Fig. 3b). One clearly can notice that the central component of the triplet is built of two hyperfine components. One can also see clearly in Figure 3a that large hyperfine splittings can be noticed in the photographic spectrum without problems. The Doppler broadened line width of the components in Figure 3b is approximately 900 MHz, corresponding to 0.01 Å. With the help of an Abbé comparator equipped with incremental length measurement systems [28] we were able to determine the wavelengths on the spectral plate also with an accuracy of ±0.01 Å. Since we are able to set our laser wavelength with the same accuracy [29], we have a quite good chance to excite the transitions belonging to up to now unknown lines just by setting the laser wavelength. In some cases, this may lead to the excitation of previously unknown levels.

As the second example we treat the wavelength region around 4 244.88 Å. Here we found first a blend situation of two lines: 4 244.83 Å and 4 244.88 Å. The first line could be explained as the transition

$$z^6\mathrm{D}^\circ_{3/2}\ (24\,739.03\ \mathrm{cm}^{-1}) - ?_{5/2}\ (48\,290.45\ \mathrm{cm}^{-1}),$$

the second one as

$$^4\mathrm{G}_{7/2}\ (24\,917.90\ \mathrm{cm}^{-1}) - ?^\circ_{9/2}\ (48\,468.96\ \mathrm{cm}^{-1}).$$

Each classification was confirmed by tuning the laser around the transition wavelength and observing fluorescence on several lines with the same upper level as the transition. Additional to the fluorescence lines coming from the upper levels of these transitions, we found a fluorescence signal when setting the monochromator to 2 681 Å. Now tuning the laser wavelength we observed a hyperfine structure which did not belong to the two lines mentioned before. So we had to assume that another, third transition is excited in this small wavelength interval. The center of gravity wavelength was determined with the help of our lambdameter to be 4 244.88 Å. By setting the laser frequency to a strong hyperfine component of this third transition, we were able to find a further fluorescence line. We determined the wavelengths of the fluorescence lines to be 2 681.80(8) Å and 2 662.06(6) Å (Fig. 2). We further were able to determine the hyperfine constants and the angular momentum (9/2 and 11/2) of the levels involved by fitting the hyperfine spectrum of the third transition. This third transition could not be explained using the already known levels energies. Since further none of the known levels has one of the A- and B-value pairs obtained, we had to conclude that the transition takes place between two up to now unknown levels.

Assuming that both fluorescence lines have as their upper levels the upper level of the excited transition, and that both fluorescence transitions take place to known energy levels, we calculated the wave number difference of the fluorescence lines. Then we were searching for two lower even parity levels having the same wave number difference. Adding the wave numbers of the fluorescence lines to the wave numbers of these levels, we could calculate the energy of the new odd level to be 52 667.30 cm^{-1}.

This level is excited by laser light, so it is connected to a new lower even level which location can be calculated (using the wave number corresponding to the wavelength 4 244.88 Å) to be 29 116.26 cm^{-1}. Nevertheless, up to now it stays unclear, whether the lower level has $J = 9/2$, $A \approx 689$ MHz, $B \approx 580$ MHz, and the upper one has $J = 11/2$, $A \approx 125$ MHz, $B \approx 3\,200$ MHz, or if the lower level has $J = 11/2$ and the upper one $J = 9/2$ (then all hyperfine constants would have the opposite sign). Fortunately, in [7] we have predicted an even level at 28 950 cm^{-1} having $A = 700$ MHz, $B = 700$ MHz. So we could assume that we have found this predicted level now at 29 116.26 cm^{-1}, having the hyperfine constants given in Table 4 (more precisely determined when confirming the existence of this level by exciting it on other transitions). This assignment is a good example of the interplay between theory and experiment.

4 Conclusion

By evaluating photographic spectra of a Ta–Ar hollow cathode lamp we could find several lines of Ta which are not mentioned in commonly used spectral tables. By exciting the transitions corresponding to such lines we were able to identify clearly the combinations belonging to these lines. Investigation of some of the lines has lead to the discovery of up to now unknown levels. It turns out that the obtained hyperfine spectra provide a powerful tool to perform fine structure investigations. Further investigations are in progress.

The authors would like to thank K. Boonpog, F. Czarnecki, O. Denke, M. Elantkowska, V. Funtov, J. Harperscheidt, A. Huth, M. Hofhaus, F. Kadelka, M. Klein, M. Müller, F. Ostermann, M. Pape, S. Plückhahn, F. Ritzmann, W. Salmhofer, M. Sauer, M. Schäfer, U. Scheurer genannt Rohling, L. Seebach, C. Zhao who all contributed valuable parts of the data presented in this paper.

References

1. A. Baier, H.-O. Behrens, G.H. Guthöhrlein, L. Windholz, Z. Phys. D **23**, 151 (1992).
2. G.H. Guthöhrlein, L. Windholz, Z. Phys. D **27**, 343 (1993).
3. G.H. Guthöhrlein, G. Helmrich, L. Windholz, Phys. Rev. A **49**, 120 (1994).
4. H. Hammerl, G.H. Guthöhrlein, M. Elantkovska, V. Funtov, G. Gwehenberger, L. Windholz, Z. Phys. D **33**, 97 (1995).
5. G.H. Guthöhrlein, H. Mocnik, L. Windholz, Z. Phys. D **35**, 177 (1995).
6. H. Mocnik, B. Arcimowicz, W. Salmhofer, L. Windholz, G.H. Guthöhrlein, Z. Phys. D **36**, 129 (1996).
7. J. Dembczynski, B. Arcimowicz, G.H. Guthöhrlein, L. Windholz, Z. Phys. D **39**, 143 (1997).
8. D. Messnarz, G.H. Guthöhrlein, Eur. Phys. J. D **12**, 269 (2000).
9. T. Schmidt, Z. Phys. **121**, 63 (1943).
10. T. Kamei, Phys. Rev. **99**, 789 (1955).
11. K. Murakawa, Phys. Rev. **110**, 393 (1958); J. Phys. Soc. Jpn **17**, 891 (1962).
12. S. Büttgenbach, G. Meisel, Z. Phys. **244**, 149 (1971).
13. K.H. Bürger, S. Büttgenbach, R. Dicke, H. Gebauer, R. Kuhnen, F. Träber, Z. Phys. A **298**, 159 (1980).
14. R. Harzer, Dissertation, Universität Bonn, 1981.
15. D.W. Duquette, D.K. Doughty, J.E. Lawler, Phys. Lett. A **99**, 307 (1983).
16. S. Salih, D.W. Duquette, J.E. Lawler, Phys. Rev. A **27**, 1193 (1983).
17. J. Persson, U. Berzinsh, T. Nilsson, M. Gustavsson, Z. Phys. D **23**, 67 (1992).
18. J. Persson, U. Berzinsh, M. Gustavsson, T. Nilsson, *13th International Conference on Atomic Physics (ICAP)*, München 1992, Abstract A-58.
19. U. Berzinsh, M. Gustavsson, J. Persson, Z. Phys. D **27**, 155 (1993).
20. A. Wannström, D.S. Gough, P. Hannaford, Z. Phys. D **22**, 723 (1992).
21. N. Ahmad, M. Akram, K.P. Gill, S.P. Asdaq, R.M. Akhtar, M. Saleem, M.A. Baig, Z. Phys. D **41**, 159 (1997).
22. P.F.A. Klinkenberg, G.J. van den Berg, J.C. van den Bosch, Physica **16**, 861 (1950).
23. G.J. van den Berg, P.F.A. Klinkenberg, J.C. van den Bosch, Physica **18**, 221 (1952).
24. Ch. Moore, *Atomic Energy Levels*, Natl. Bur. Stand. (U.S.) Circ. No. 467 (Washington, D.C., U.S. GPO, 1958), Vol. III.
25. W.F. Meggers, C.H. Corliss, B.F. Scribner, Natl. Bur. Stand. (U.S.), Monograph 32, Part I, 1961.
26. G.R. Harrison, *Massachusetts Institute of Technology Wavelength tables* (The M.I.T. press, 1985).
27. W.F. Meggers, C.H. Corliss, B.F. Scribner, Natl. Bur. Stand. (U.S.), Monograph 145, Part I, 1975.
28. C. Neureiter, L. Windholz, Jenaer Rundschau 1981/4, 147.
29. G. Pfeifer, C. Neureiter, L. Windholz, Exper. Tech. Phys. **39**, 161 (1991).
30. S. Kröger (presently at Technische Universität Berlin, Institut für Atomare und Analytische Physik, Hardenbergstraße 36, D-10623 Berlin), private communication.